

Modelling of Multi-Tier Handover in LiFi Networks

Ahmet Burak Ozyurt¹, Ilenia Tinnirello², Wasu O. Popoola¹

¹Institute for Digital Communications, School of Engineering, The University of Edinburgh, EH9 3JL, Edinburgh, United Kingdom. Email: {a.b.ozyurt, w.popoola}@ed.ac.uk

²Engineering Department, University of Palermo, Italy. Email: {ilenia.tinnirello}@unipa.it

Abstract—This paper presents a two-tier LiFi network and analyses the cross-tier handover rate between the primary and secondary cells. Based on the semiangle at half illuminance of the primary and secondary cells, we propose coverage model for the secondary cells. Using stochastic geometry, closed-form expressions are derived for the cross-tier handover rate and sojourn time in terms of the received optical signal intensity, time-to-trigger and user mobility. The analytical models are validated with simulation results.

Keywords—Multi-tier, mobility, handover, LiFi, visible light communication.

I. INTRODUCTION

The significant increase in demand for wireless communication, compels researchers look ahead to the next-generation technologies. If we consider that approximately 80 percent of wireless data traffic originates or terminates within a building, new global research should focus on this critical indoor wireless gap [1]. 2G and 3G connectivity still enable the majority of internet of things (IoT) applications, but the number of short-range IoT connections will increase by 13 percent annually and reach close to 20 million connections at the end of the 2025 [2], [3]. Satisfying these demands is highly desirable for future wireless technologies. LiFi -a light spectrum based wireless systems- is a critical technology because it offers huge unlicensed spectrum, physical layer security, low-cost, high data rate, and can potentially serve as a complementary technology to the current radio frequency (RF) based systems [4].

From the very beginning of wireless networks, handover or mobility management has been one of the most investigated research areas in communication engineering. The cell radius, which was previously expressed in kilometres, has reduced a few meters in LiFi. Especially, when multiple tiers are considered in the wireless networks, mobility management becomes more complex than before. This small radius and multiple tiers have posed a lot of challenges in terms of user mobility management [5].

The current LiFi network studies focus on the vertical handover schemes, namely hybrid RF-LiFi networks [6]. In [7], the probability of vertical handover is investigated for a user with random rotations in the hybrid RF-LiFi

networks. Also, the Markov decision process is proposed for improving vertical handovers [8]. Another vertical handover scheme, which predicts the parameters in terms of access delays, data size and interruption duration, was proposed in [9]. These parameters are utilized by the system to make handover decisions. Chowdhury and Katz investigated the performance of the hybrid RF-LiFi hot-spot networks in a mobile scenario [10]. A fuzzy logic based vertical handover algorithms were proposed to solve the line-of-sight (LoS) blocking [11]. Due to a change of air interfaces, a vertical handover usually needs a much longer processing time than a horizontal handover [12]. Also, the RF system has a lower system capacity than LiFi, and an excessive number of RF users would cause a substantial decrease in throughput. For these reasons, dynamic load balancing, resource allocation, and a number of optimization have been mostly investigated in vertical handover schemes [6].

However, the main problem is in horizontal handover among LiFi access points (APs). In the horizontal handover, the received signal strength (RSS) parameter in the optical domain is exploited to develop an RSS-based handover mechanism for mobile LiFi users. The user is mainly served by an AP (i.e., luminary) from which it gets the strongest signal. When the user moves towards the cell edge, the received signal drops and a handover has to be executed. In some cases, the effects of frequency partitioning and rotation for connected user equipment (UE) is also evaluated in regards to RSS value [13]. The handover skipping (HS) technique (based on RSS) which disregarded some adjacent cells is proposed and compared with the standard handover. The vast majority of algorithms use the RSS parameter to reach the final decision. The foregoing horizontal handover studies focus on one tier system in LiFi networks. They do not consider the realistic scenarios of multi-tier ultra-dense LiFi networks. Although, cross-tier mobility management is a well-studied subject in RF heterogeneous networks. LiFi networks have unique features that make its cross-tier mobility different to that in RF.

Multiple tiers in ultra-dense LiFi networks is representative of the realistic scenario. The different tiers can be considered as the different light sources such as the ceiling, floor, and desk lamps. Also, when we take the very small coverage of LiFi tiers into consideration, the mobility management problem becomes inevitable. Thus, the study of handover is of great importance in multi-tier LiFi networks. In this study, a multi-tier LiFi networks is studied. A realistic case for such a system is an office environment with two different types of light sources as suggested in the IEEE 802.11bb Task Group on Light Communications [14]. However, the authors are not aware of any reported

This work is funded by the European Union's Horizon 2020 research and innovation programme under the Marie Skłodowska Curie grant agreement No. 814215 titled ENLIGHT'EM: European Training Network in Low-Energy Visible Light IoT Systems: <https://enlightem.eu/>

theoretical or practical work on multi-tier concept in LiFi networks except our previous work [15]. In our previous work, we consider the various scenarios of semiangle at half illuminance of the transmitters and ping-pong rates as different than the current study.

In LiFi, the cell size is considerably smaller than in RF and therefore handover rate, TTT, sojourn time within a cell and prevention of unnecessary back and forth handover via the estimation of the ping-pong rate are all vital mobility management metrics. These are the metrics that we have studied for a LiFi configuration with a number of light sources. In addition to the small coverage area of LiFi, the issue of mobility management is made more desirable due to the dissimilar distribution of light intensity by the different light sources. This is the motivation for considering received optical intensity (ROI) in our mobility management work.

In this paper, we investigate the cross-tier mobility management in ultra-dense LiFi networks using stochastic geometry. The contributions are as follows: 1) For the first time in literature, we introduce the multiple-tiers concept in the LiFi networks for enhancing mobility management in a realistic environment; 2) we propose a secondary cell coverage scenario that is based on the half-angle of the primary and secondary AP light sources; 3) closed-form expressions are presented for cross-tier handover rate and sojourn time as functions of time to trigger (TTT), AP intensities, and user velocity; 4) the closed-form analytical results are verified through simulations. The effect of system parameters such as TTT and user velocity are explained on the mobility performance, which could provide deeper insight for realistic LiFi network planning.

II. SYSTEM MODEL

In this section, the network model used is presented. At first, the LiFi network placement model is realized according to multi-tier concept. The two tiers are distinguished by their transmission power and spatial density. The primary access points (PAPs) and the secondary access points (SAPs) are deployed using a poisson point process (PPP) model on the Poisson-Voronoi tessellation (PVT). Secondly, the LiFi channel model used in the analytical calculations is briefly discussed and the user equipment (UE) movement model is presented as well.

A. Network Model

In real scenarios, the LiFi networks typically contain a large number of ‘statically random’ APs, such as ceiling luminaries, desktop lamps, and even LED screens [5]. Therefore, the use of a regular/deterministic model for the positioning of these light sources will be unrealistic. Hence, spatial point process provides more accurate and tractable solutions for such a LiFi network modelling [16].

The point process is defined as a random group of many points that can be counted with a multiple probability, while the PPP is the number of points in a set with a Poisson distribution having parameter λ (mean intensity) [17]. A point process $\Phi = \{x_{(i)} : i = 1, 2, \dots\} \subset \mathbb{R}^d$ is a PPP if and only if the number of the points in any compact set $B \subset \mathbb{R}^d$ is a Poisson random variable. The \mathbb{R}^d is referred to as d dimensional space in real plane. For every compact set B , $N(B)$ has a Poisson distribution with mean $\lambda|B|$ and

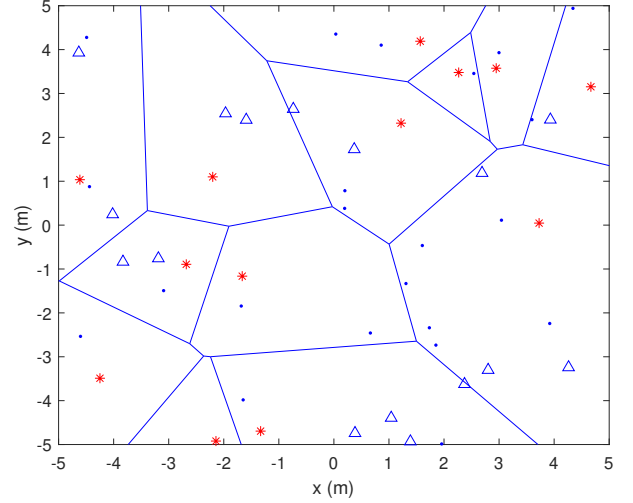


Fig. 1: PVT ultra-dense LiFi network with the primary access points (red stars), the secondary access points (blue triangles) and mobile users (blue dots).

$|\cdot|$ is the Lebesgue measure of set B . Then, any measurable set B defines:

$$P\{\Phi(B) = t\} = \frac{(\lambda|B|)^t}{t!} \exp(-\lambda|B|). \quad (1)$$

In this work, the set B is considered as a two-dimensional Euclidean space and the APs are distributed on the Voronoi tessellation according to the PPP indicated with Φ and intensity λ [18]. The Voronoi tessellation is a partition of the plane into n convex polytopes. Each partition contains one generator such that every point in the partition is closer to its own generator than any other generator [19]. The APs in the primary tier p and secondary tier s are distributed following two independent PPPs with intensities λ_p and λ_s respectively. Through this approach, the network system design becomes more realistic and appropriate for optimization studies including the investigation of mobility. Figure 1 shows the network deployment where the PAPs are indicated by red stars, the SAPs are indicated by blue triangles, and the mobile users are showed by blue dots in a 2-D coordinate system.

B. LiFi Channel Model

Mobility management process in LiFi networks is based on the Received Optical Intensity (ROI). Namely, the measured ROIs are the principal criteria for initiating a handover process. In this paper, only LoS is considered for LiFi and the effect of multiple reflections from the walls and human shadowing are ignored. It is shown in [20] that the reflection paths have an insignificant effect on the LiFi APs that are sufficiently far away from the network boundaries. Under this assumption, the ROI of users from the APs in tier i ($i = p, s$) is given by the product of the transmitted power and the path loss [21]:

$$\text{ROI}_i(d_{i,u}) = P_i \frac{(m_i + 1)A_r}{2\pi d_{i,u}^2} \cos^{m_i}(\varphi_i) T_s g(\psi_i) \cos(\psi_i), \quad (2)$$

where $d_{i,u}$ denotes the distance from the user to an AP in tier i , P_i is the transmitted power, A_r is the receiver effective area, T_s is the filter transmission, $g(\psi_i)$ and ψ_{con} are the concentrator gain and field-of-view (FOV), respectively, and m_i is the Lambertian index defined as [21]:

$$m_i = -\frac{\ln(2)}{\ln[\cos(\varphi_{1/2})]}, \quad (3)$$

where $\varphi_{1/2}$ is the semiangle at half illuminance of the transmitter. The gain of the optical concentrator at the receiver is defined by [21]:

$$g(\psi) = \begin{cases} n^2 / \sin^2(\psi_{con}), & \text{if } 0 < \psi \leq \psi_{con} \\ 0, & \text{if } \psi_{con} \leq 0, \end{cases} \quad (4)$$

where n is the refractive index.

C. Mobility Model

In this paper, we used an improved Random Way Point (RWP) mobility model which is proposed in [22] due to its simplicity in modelling movement patterns of mobile nodes.

In this model, UEs move in a limited domain such as \mathcal{A} . At each time, the random destination points (referred to as waypoint) are chosen as uniformly distributed in \mathcal{A} . Then, the UE follows a straight line between its current waypoint to the newly selected waypoint at the decided constant velocity. The process repeats at each destination point and the user can have an optional random pause time. We acknowledge that human movement has very complex temporal and spatial correlations and its nature has not been fully understood and therefore cannot be perfectly modelled [23], [24]. Human movement within a space will be impacted by the presence of physical objects within that space. Modeling such a movement is highly complex and will depend on the given scenario and environment. Developing such a model is outside the scope of this work. Instead, we assume that the user movement is random and follows the RWP mobility model. The RWP model is tractable and provides a basis to evaluate mobility management in LiFi. By using this model, it is now possible to analyze the impact of user mobility on LiFi networks thereby providing an insight into designing a reliable LiFi network. The framework that we present can be used/extended to any other user mobility model.

The proposed RWP mobility model can be described by an infinite sequence of quadruples $\{(\mathbf{X}_{k-1}, \mathbf{X}_k, V_k, S_k)\}_{k \in K}$, where k denotes the k th movement period. During the k th movement, \mathbf{X}_{k-1} denotes the starting waypoint, \mathbf{X}_k denotes the target waypoint, V_k denotes the velocity, and S_k denotes the pause time at the waypoint \mathbf{X}_k . Given the starting waypoint \mathbf{X}_{k-1} , a homogeneous PPP $\Phi_u(k)$ with intensity λ_u is independently generated and then the nearest point in $\Phi_u(k)$ is selected as the target waypoint. That is:

$$\mathbf{X}_k = \arg \min_{\mathbf{x} \in \Phi_u(k)} |\mathbf{x} - \mathbf{X}_{k-1}|. \quad (5)$$

Therefore, denoting the transition length of the k th movement as $L_k = |\mathbf{X}_{k-1} - \mathbf{X}_k|$, the cumulative distribution function (CDF) of L_k can be written as [25]:

$$P_{L_k}(L_k \leq l) = 1 - \exp(-\lambda_u \pi l^2), \quad l > 0 \quad (6)$$

This is the probability that L_k is smaller than a given distance l is the probability that the points in the area

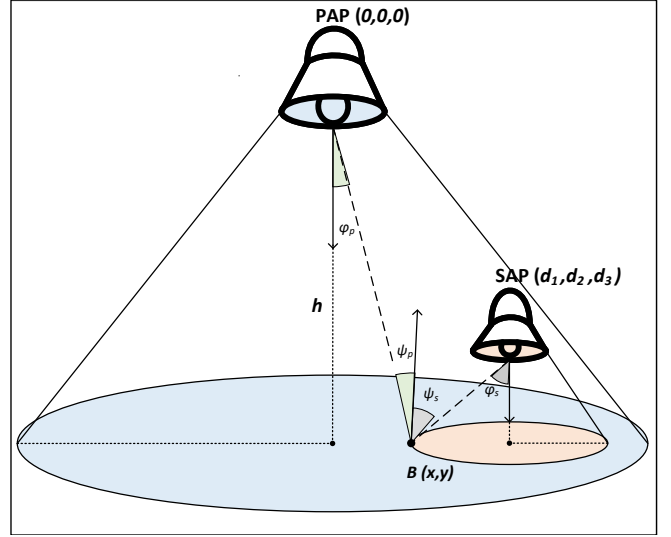


Fig. 2: The multi-tier LiFi network with the primary access point and the secondary access point.

(πl^2). The transition lengths are Rayleigh distributed [26]. Besides, velocity V_k and pause time S_k are independent, identically distributed (i.i.d.) with distributions $P_V(\cdot)$ and $P_S(\cdot)$, respectively.

III. ANALYTICAL MODEL FOR SECONDARY CELL COVERAGE AREA

Generally, a network consists of multiple cells that are adjacent to one another. The cell coverage area is delimited by the adjacent cells. In other words, borders among cells are determined by the received signal which is ROI in LiFi [27]. In this paper, all UEs faces are directed upward and APs share an equal semiangle at half illuminance for sake of simplicity and clarity. Also, it is considered that UEs and APs are moving only in a 2D plane. Thus, their height from the ground has been taken as constant.

When the P2S (primary-to-secondary) cross-tier handover process is taken into account, it is assumed that the user is initially deployed inside the coverage of the PAP such as in Figure 2. In multi-tier LiFi networks, PAPs are deployed with low spatial density, high transmit optical power and wider coverage area. On the other hand, SAP, will be a set of other light sources, with lower and smaller coverage area than the PAP. The SAP can be very localised and could support higher data rates. In addition, the PAP is considered as an umbrella tier and the SAPs are located under this umbrella. Namely, each SAP is covered by a PAP. It is assumed that the PAPs and the SAPs are both connected to the same backbone and coordinated. Without loss of generality, we assume that a typical PAP l_p is located at the origin, and a SAP l_s is located at position $\mathbf{x}_s(d_1, d_2, d_3)$. According to the ROI, the coverage boundary of the SAP l_s can be determined as,

$$B = \{(x, y) \in \mathbb{R}^2 \mid \text{ROI}_p(d_{p,u}) = \text{ROI}_s(d_{s,u})\}. \quad (7)$$

Thus, a set of equal ROI points in (7) form the coverage boundary of the SAP. These points will help in calculating the mobility management parameters in a LiFi network. For

a user located at $(x, y) \in \mathbb{R}^2$ and the height from the ground is h , the distance from user to the PAP, and the SAP are given, respectively, by,

$$d_{p,u} = \sqrt{x^2 + y^2 + h^2}, \quad (8)$$

$$d_{s,u} = \sqrt{(x - d_1)^2 + (y - d_2)^2 + (h - d_3)^2}. \quad (9)$$

In addition, $\cos(\varphi_p) = \cos(\psi_p) = \frac{h}{\sqrt{x^2 + y^2 + h^2}}$ and $\cos(\varphi_s) = \cos(\psi_s) = \frac{h - d_3}{\sqrt{(x - d_1)^2 + (y - d_2)^2 + (h - d_3)^2}}$ are considered because UEs faces are assumed to be directed upward. By substituting (8) and (9) into (7), we obtain,

$$W \cdot (x^2 + y^2 + h^2)^{\hat{m}} - [(x - d_1)^2 + (y - d_2)^2 + (h - d_3)^2] = 0 \quad (10)$$

where, $W = \left(\frac{P_s(m_s+1)(h-d_3)^{m_s+1}}{P_p(m_p+1)h^{m_p+1}} \right)^{\frac{2}{m_s+3}}$, $\hat{m} = \frac{m_p+3}{m_s+3}$. As assumed that at the beginning of Section III, both the PAP and the SAP share an equal Lambertian index ($m_p = m_s$), \hat{m} equals 1. Thus, the defined function in (10), can be simplified into a circular equation. The corresponding center $\mathbf{x}_c = (x_c, y_c)$ as well as the radius R_c is calculated as:

$$\mathbf{x}_c = \left(\frac{d_1}{1-W}, \frac{d_2}{1-W} \right) \quad (11)$$

$$R_c = \sqrt{\frac{W(d_1^2 + d_2^2)}{(1-W)^2} + \frac{Wh^2 - (h - d_3)^2}{(1-W)}}. \quad (12)$$

IV. CROSS-TIER MOBILITY ANALYSES FOR RESILIENT LIFI

Network densification through multiple-tiers is an inescapable part of next-generation LiFi systems. However, the handover rate is higher in smaller and denser cells, and handover rate directly affects the network signalling overhead. Among the different types of handover, the cross-tier handover showed the highest handover failure rate [28], [29]. The P2S handover rate can be defined as follows [13]:

$$H = H_t \times P(S > TTT), \quad (13)$$

where the P2S handover trigger rate H_t represents the number of times that the UE that resides in a primary tier moves across a secondary tier coverage boundary in a unit time. $P(S > TTT)$ is the probability that the UE's sojourn time S inside the secondary tier coverage area is larger than the TTT duration.

According to RWP mobility model, the movement trace of the UEs can be divided into infinite parts. Thus, the P2S handover trigger rate can be defined as the expected number of triggered P2S handovers $E[N]$ during one movement period divided by the expected period of time $E[T]$. So, the P2S handover trigger rate is expressed as follows,

$$H_t = \frac{E[N]}{E[T]}. \quad (14)$$

The trajectory line in the k -th movement period is defined with the two successive waypoints, \mathbf{X}_{k-1} and \mathbf{X}_k . Thus, we assume that user follows the movement traces of $\dots, \mathbf{X}_{k-1}, \mathbf{X}_k, \dots$. We can derive the number of triggered P2S handovers by calculating the number of intersection between the secondary tier boundaries and the UE's trajectory line, denoted as $L(\mathbf{X}_{k-1}, \mathbf{X}_k)$.

Let $l_{\mathbf{x}_i}$ denote the coverage area delimited by the SAP. According to (12), $l_{\mathbf{x}_i} = C(\mathbf{x}_i, R_i)$, where R_i is the radius of the SAP. We can assume that $L_{(+R_i)}$ can be the set of points laying in the intersection of the following two conditions:

- 1) At most R_i units distant from the line segment $L(\mathbf{X}_{k-1}, \mathbf{X}_k)$, and
- 2) At least R_i units distant from the start point \mathbf{X}_{k-1} , which will be expressed as,

$$L_{(+R_i)} = \{\mathbf{x} \in \mathbb{R}^2 \mid D(\mathbf{x}, L(\mathbf{X}_{k-1}, \mathbf{X}_k)) \leq R_i \cap D(\mathbf{x}, \mathbf{X}_{k-1}) \geq R_i\}, \quad (15)$$

where $D(\mathbf{x}, L(\mathbf{X}_{k-1}, \mathbf{X}_k))$ is the shortest Euclidean distance from \mathbf{x} to the UE's trajectory line $L(\mathbf{X}_{k-1}, \mathbf{X}_k)$, and

$$|L_{(+R_i)}| = 2|L(\mathbf{X}_{k-1}, \mathbf{X}_k)|R_i. \quad (16)$$

Assume the segment $L(\mathbf{X}_{k-1}, \mathbf{X}_k)$ is fixed and moves towards the circle center. If the circle center falls within the coverage of $L_{(+R_i)}$, the segment intersects with the secondary cell coverage circle. Based on geometry probability theory, the probability that an P2S handover event occurs in the SAP $l_{\mathbf{x}_i}$ during the k th period is $|L_{(+R_i)}|/|\mathcal{A}|$, where $|L_{(+R_i)}|$ has been derived in (16). Averaged over the entire probability space, the expected P2S handover trigger rate for one target SAP is derived as follows,

$$\begin{aligned} P_{ho_t} &= \int_0^\infty \int_0^\infty \frac{|L_{(+R_i)}|}{|\mathcal{A}|} f_{L(\mathbf{x}_{k-1}, \mathbf{x}_k)}(l) f_{R_i}(r) dl dr \\ &= \frac{2}{|\mathcal{A}|} E[|L(\mathbf{X}_{k-1}, \mathbf{X}_k)|] E[R_i] \\ &= \frac{2}{|\mathcal{A}|} \frac{1}{2\sqrt{\lambda_u}} \sqrt{\frac{WE[X_{s2p}]^2}{(1-W)^2} + \frac{Wh^2 - (h - d_3)^2}{(1-W)}} \\ &= \frac{1}{|\mathcal{A}|\lambda_u} \sqrt{\frac{W}{4\lambda_p(1-W)^2} + \frac{Wh^2 - (h - d_3)^2}{(1-W)}} \quad (17) \end{aligned}$$

where $f_{L(\mathbf{x}_{k-1}, \mathbf{x}_k)}(l)$ is the probability density function (PDF) of the UE's transition length and it follows Rayleigh distribution because of RWP specifications. Also, $f_{R_i}(r)$ is the PDF of the secondary cell radius. In fact, Rayleigh distribution of the RWP ensures that $E[|L(\mathbf{X}_{k-1}, \mathbf{X}_k)|] = \frac{1}{2\sqrt{\lambda_u}}$. In addition, it is obtained that $E[X_{s2p}] = \frac{1}{2\sqrt{\lambda_p}}$ based on stochastic geometry.

In this manner, the expected number of triggered P2S handovers during the n th movement period is given by:

$$E[N] = \lambda_s |\mathcal{A}| P_{ho_t}. \quad (18)$$

On the other side, we note that $E[T] = E[T_s] + E[T_t]$, where $E[T_s]$ and $E[T_t]$ are the mean pause time and the mean transition time, $E[T_t] = E[|L(\mathbf{X}_{k-1}, \mathbf{X}_k)|/v]$. By combining (14) and (18), the closed-form expression of the P2S handover trigger rate with considering user velocity

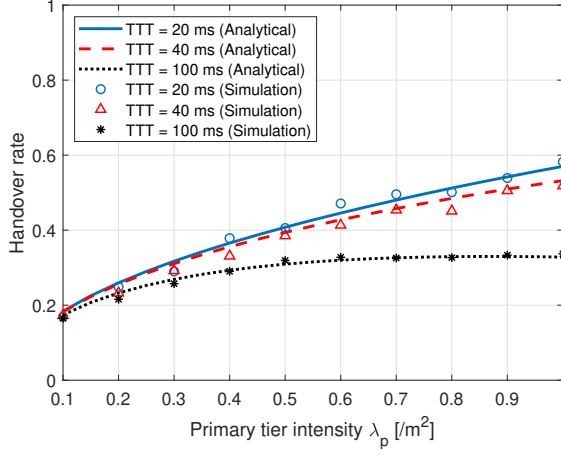


Fig. 3: P2S handover rate.

becomes:

$$\begin{aligned}
 H_t &= \frac{\lambda_s v}{\sqrt{\lambda_u v E[T_t]} + \sqrt{\lambda_u v E[T_s]}} \\
 &\times \sqrt{\frac{W}{4\lambda_p(1-W)^2} + \frac{Wh^2 - (h-d_3)^2}{(1-W)}} \\
 &= \frac{2\lambda_s v}{1 + 2\sqrt{\lambda_u v E[T_s]}} \sqrt{\frac{W}{4\lambda_p(1-W)^2} + \frac{Wh^2 - (h-d_3)^2}{(1-W)}}. \quad (19)
 \end{aligned}$$

According to (14), cross-tier handover will happen when the UE sojourn time S inside that secondary cell is larger than TTT duration. After obtaining handover trigger rate, we need to find the probability of sojourn time which is larger than TTT.

Firstly, the expected trajectory length inside a secondary cell with radius R_c is given as,

$$L_c(R_c) = \frac{\pi}{2} R_c. \quad (20)$$

By replacing R_c with X_{p2m} in (12), the sojourn time inside a secondary cell is given as:

$$S = \frac{L_c(R_c)}{v} = \frac{\pi}{2v} \sqrt{\frac{W X_{s2p}^2}{(1-W)^2} + \frac{Wh^2 - (h-d_3)^2}{(1-W)}}. \quad (21)$$

The CDF of X_{p2m} represents the probability that the handover UE's sojourn time inside the secondary cell is larger than TTT,

$$\begin{aligned}
 P(S \geq TTT) &= \exp \left\{ -\lambda_p \pi \frac{(1-W)^2}{W} \right. \\
 &\times \left[\left(\frac{2vTTT}{\pi} \right)^2 - \left(\frac{Wh^2 - (h-d_3)^2}{(1-W)} \right) \right] \left. \right\} \quad (22)
 \end{aligned}$$

By plugging (19) and (22) into (13), the closed-form expression of the expected P2S handover is derived below,

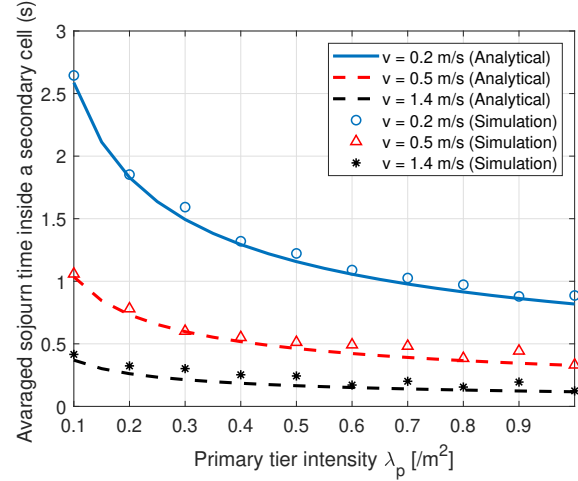


Fig. 4: Average sojourn time inside a secondary cell by analyses and simulation.

this denotes the P2S handover rate,

$$\begin{aligned}
 H &= \frac{2\lambda_s v}{1 + 2\sqrt{\lambda_u v E[T_s]}} \sqrt{\frac{W}{4\lambda_p(1-W)^2} + \frac{Wh^2 - (h-d_3)^2}{(1-W)}} \\
 &\times \exp \left\{ -\lambda_p \pi \frac{(1-W)^2}{W} \right. \\
 &\times \left[\left(\frac{2vTTT}{\pi} \right)^2 - \left(\frac{Wh^2 - (h-d_3)^2}{(1-W)} \right) \right] \left. \right\}. \quad (23)
 \end{aligned}$$

V. NUMERICAL RESULTS AND DISCUSSIONS

In this section, we discuss the analytical results of P2S cross-tier handover performance metrics and compare with the simulation results. For the purpose of illustration, we consider a room with dimensions: $10 \times 10 \times 3$ m³. The semiangle at half illuminance of the transmitters is selected as equal to 60°. Furthermore, $P_p = 25P_s$ is assumed as the relationship among transmit powers for this illustration scenario. The height of UEs and SAPs from the ground is taken as 0.75 m and 1.2 m, respectively.

In Figures 3 and 4, we present simulation results to verify the analytical results of the P2S cross-tier handover performance metrics which are derived in Section IV. The movement of an UE is based on the mobility model given in Section II. We consider a two-tier ultra-dense LiFi network deployment scenario, where the PAPs and the SAPs are distributed using two independent homogenous PPPs, Φ_p , Φ_s , with intensities λ_p and λ_s , respectively. Additionally, $\lambda_s = 2\lambda_p$ is assumed and UEs velocity is considered as $v = 1.4$ m/s. Also, according to 3GPP TS 36.839 specification, TTT timer has 4 typical values. These values are 40 ms, 80 ms, 160 ms, and 480 ms respectively. However, these values must be lower in LiFi. Thus, TTT values are taken into account as 20 ms, 40 ms, and 100 ms in the simulations.

Figure 3 depicts the P2S handover rate versus different primary cells intensity λ_p . It is clear that the handover rate increases within the denser deployment. This is because the secondary cell deployment gets denser as λ_p increases,

which means that the cross-tier handover will be triggered more. On the other hand, the handover rate decreases as TTT values increase because users are less likely to enter a new secondary cell. In Figure 4, the average sojourn time inside a secondary cell decreases with high velocity and denser deployment. As expected, higher UE velocity is a reason for shorter residence time in a secondary cell and the coverage area of a SAP decreases with high intensity.

The results show that the analytical expressions match the simulations quite well. The above simulation results not only validate our analytical results in Section IV, but also provide deeper knowledge for mobility enhancement in ultra-dense LiFi networks. For instance, if we have a value of the SAP intensity in a certain area, we can estimate the velocity of the user by applying the analytical expression of the cross-tier handover rate. Also, these analytical expressions can be beneficial for increasing the positioning accuracy such as using the sojourn time when the results are not enough or the position error is very large. In the case of TTT and APs deployment being fixed, various mobility management strategies can be applied to UEs with different velocities. For example, high mobility users can always connect to the PAPs and avoid P2S handover due to its possible high handover rate.

VI. CONCLUSION

In this paper, the key performance metrics in multi-tier LiFi networks are analyzed for handover from the primary tier to the secondary tier. Based on semiangle at half illuminance, we presented the analytical model for the coverage areas of the SAP. We derived closed form expressions for the P2S cross-tier handover and sojourn time as functions of the system parameters. These expressions show that TTT, AP intensity of each tier, and user velocity have a critical impact on the mobility management in LiFi. In addition, simulation results are presented to validate the theoretical models presented. The findings will be valuable in practical LiFi deployment and planning as well as handover optimization in multi-tier networks.

REFERENCES

- [1] Cisco, "Cisco service provider-wi-fi: A platform for business innovation and revenue generation," *CISCO White Paper*, ID:1458684054151755, Nov. 2012.
- [2] A. B. Ozyurt, M. Basaran, M. Ardanuc, L. Durak-Ata, and H. Yanikomeroglu, "Intracell frequency band exiling for green wireless networks: Implementation, performance metrics, and use cases," *IEEE Vehicular Technology Magazine*, vol. 16, no. 2, pp. 31–39, 2021.
- [3] A. B. Özyurt, A. Hız, and L. D. Ata, "Energy-efficient utilization of different frequency bands for green cellular networks," in *2018 26th Signal Processing and Communications Applications Conference (SIU)*, 2018, pp. 1–4.
- [4] Z. Ghassemlooy, W. Popoola, and S. Rajbhandari, *Optical wireless communications: system and channel modelling with Matlab®*. CRC press, 2019.
- [5] H. Haas, L. Yin, Y. Wang, and C. Chen, "What is lifi?" *Journal of Lightwave Technology*, vol. 34, no. 6, pp. 1533–1544, 2016.
- [6] F. Wang, Z. Wang, C. Qian, L. Dai, and Z. Yang, "Efficient vertical handover scheme for heterogeneous vlc-rf systems," *IEEE/OSA Journal of Optical Communications and Networking*, vol. 7, no. 12, pp. 1172–1180, 2015.
- [7] A. A. Purwita, M. D. Soltani, M. Safari, and H. Haas, "Handover probability of hybrid lifi/rf-based networks with randomly-oriented devices," in *2018 IEEE 87th Vehicular Technology Conference (VTC Spring)*, 2018, pp. 1–5.
- [8] F. Wang, Z. Wang, C. Qian, L. Dai, and Z. Yang, "Efficient vertical handover scheme for heterogeneous vlc-rf systems," *IEEE/OSA Journal of Optical Communications and Networking*, vol. 7, no. 12, pp. 1172–1180, 2015.
- [9] S. Liang, H. Tian, B. Fan, and R. Bai, "A novel vertical handover algorithm in a hybrid visible light communication and lte system," in *2015 IEEE 82nd Vehicular Technology Conference (VTC2015-Fall)*, 2015, pp. 1–5.
- [10] H. Chowdhury and M. Katz, "Data download on move in indoor hybrid (radio-optical) wlan-vlc hotspot coverages," in *2013 IEEE 77th Vehicular Technology Conference (VTC Spring)*, 2013, pp. 1–5.
- [11] J. Hou and D. C. O'Brien, "Vertical handover-decision-making algorithm using fuzzy logic for the integrated radio-and-ow system," *IEEE Transactions on Wireless Communications*, vol. 5, no. 1, pp. 176–185, 2006.
- [12] 3GPP, "Requirements for evolved utra (e-utra) and evolved utran (e-utran)," 2009.
- [13] M. D. Soltani, H. Kazemi, M. Safari, and H. Haas, "Handover modeling for indoor lifi cellular networks: The effects of receiver mobility and rotation," in *2017 IEEE Wireless Communications and Networking Conference (WCNC)*, 2017, pp. 1–6.
- [14] M. Uysal, F. Miramirkhani, T. Baykas, and K. Qaraqe, "IEEE 802.11 bb reference channel models for indoor environments," Tech. Rep., 2018.
- [15] A. B. Ozyurt and W. O. Popoola, "Mobility management in multi-tier lifi networks," *IEEE/OSA Journal of Optical Communications and Networking*, vol. 13, no. 9, pp. 204–213, 2021.
- [16] S. N. Chiu, D. Stoyan, W. S. Kendall, and J. Mecke, *Stochastic geometry and its applications*. John Wiley & Sons, 2013.
- [17] G. Last and M. Penrose, *Lectures on the Poisson process*. Cambridge University Press, 2017, vol. 7.
- [18] A. R. Khamesi and M. Zorzi, "Energy and area spectral efficiency of cell zooming in random cellular networks," in *Global Communications Conference (GLOBECOM)*, 2016 IEEE. IEEE, 2016, pp. 1–6.
- [19] Q. Du, V. Faber, and M. Gunzburger, "Centroidal voronoi tessellations: Applications and algorithms," *SIAM review*, vol. 41, no. 4, pp. 637–676, 1999.
- [20] C. Chen, D. A. Basnayaka, and H. Haas, "Downlink performance of optical attocell networks," *Journal of Lightwave Technology*, vol. 34, no. 1, pp. 137–156, 2016.
- [21] Z. Ghassemlooy, L. N. Alves, S. Zvanovec, and M.-A. Khalighi, *Visible light communications: theory and applications*. CRC press, 2017.
- [22] X. Lin, R. K. Ganti, P. J. Fleming, and J. G. Andrews, "Towards understanding the fundamentals of mobility in cellular networks," *IEEE Transactions on Wireless Communications*, vol. 12, no. 4, pp. 1686–1698, 2013.
- [23] M. C. Gonzalez, C. A. Hidalgo, and A.-L. Barabasi, "Understanding individual human mobility patterns," *nature*, vol. 453, no. 7196, pp. 779–782, 2008.
- [24] C. Song, T. Koren, P. Wang, and A.-L. Barabási, "Modelling the scaling properties of human mobility," *Nature physics*, vol. 6, no. 10, pp. 818–823, 2010.
- [25] S. Bandyopadhyay, E. J. Coyle, and T. Falck, "Stochastic properties of mobility models in mobile ad hoc networks," *IEEE Transactions on Mobile Computing*, vol. 6, no. 11, pp. 1218–1229, 2007.
- [26] E. Hyttia, P. Lassila, and J. Virtamo, "Spatial node distribution of the random waypoint mobility model with applications," *IEEE Transactions on Mobile Computing*, vol. 5, no. 6, pp. 680–694, 2006.
- [27] M. D. Soltani, A. A. Purwita, Z. Zeng, H. Haas, and M. Safari, "Modeling the random orientation of mobile devices: Measurement, analysis and lifi use case," *IEEE Transactions on Communications*, vol. 67, no. 3, pp. 2157–2172, 2019.
- [28] D. Lopez-Perez, I. Guvenc, and X. Chu, "Mobility management challenges in 3gpp heterogeneous networks," *IEEE Communications Magazine*, vol. 50, no. 12, pp. 70–78, 2012.
- [29] A. B. Ozyurt, M. Basaran, and L. Durak-Ata, "Impact of self-configuration on handover performance in green cellular networks," in *2018 Advances in Wireless and Optical Communications (RTUWO)*, 2018, pp. 194–197.